

Figure 2. Ultraviolet spectra of **1** in solid nitrogen with 2% CO: (a) after irradiation at 20 K and (b) after warming to 40 K.

Carbon monoxide labeled with ^{13}C and separately with ^{18}O were reacted with dimethylsilylene and produced infrared bands with the expected shift in wavenumber. The isotopic shift data along with calculated wavenumbers are given in Table I. In addition to the 1962-cm^{-1} band one other weaker infrared band appears at 765 cm^{-1} . This band shows no shift with either ^{13}C or ^{18}O labeling of CO and appears to be a methyl rocking vibration.

A UV-vis band with maximum absorbance at 342 nm appears under the same reaction conditions that give rise to the 1962-cm^{-1} band. This band was observed in argon and nitrogen matrices as well as in a matrix of pure CO with **1**. See Figure 2. In inert matrices the characteristic 450-nm band of dimethylsilylene is present, but in pure CO the only band observed is that at 342 nm .

When **1** is dissolved in 3-methylpentane, frozen in liquid nitrogen, and irradiated, the matrix turns yellow, and the 450-nm band appears. With the addition of 300 Torr of CO to the sample cell before freezing irradiation of the glass results in a spectrum displaying both the 342-nm and 450-nm bands. As the glass remains at 77 K for several hours following irradiation the 342-nm band grows in intensity, while the 450-nm band diminishes—a result of the limited mobility of CO in the 3-methylpentane glass. Analysis of products of the 3-methylpentane glass reaction by GC-mass spectrometry gave no products attributable to a structure incorporating CO bonded with dimethylsilylene.

Our initial expectation was that the reaction product represented a Lewis acid-base adduct with the C lone pair of CO forming a coordinate covalent bond with the empty p orbital on silicon, which would assume a pyramidal geometry: $(\text{CH}_3)_2\text{Si} \leftarrow \text{C} \equiv \text{O}$. Formation of the ketene would formally require loss of one C–O π bond to form the Si–C π bond—a seemingly endothermic process. However MNDO/AM1 and ab initio calculations⁸ give quite different structures for optimized geometries. Both AM1 and MNDO calculations have a minimum energy for the silaketene geometry. Calculated geometries have a Si–C bond length of 1.625 \AA (MNDO) and 1.644 \AA (AM1), clearly in the range of Si=C double bond lengths.⁹ Ab initio calculations with a 3-21G basis set give a lowest energy structure which is pyramidal at Si with an Si–C bond length of 2.891 \AA and a C–Si–CO angle of 89° , while the silaketene structure is 84 kJ/mol higher in energy

than the pyramidal structure. The CO bond lengths are 1.185 \AA (MNDO) and 1.125 \AA (3-21G) for the adduct compared with 1.163 \AA (MNDO), 1.129 \AA (3-21G), and 1.128 \AA (experimental) for CO. The data in Table I indicate that MNDO and AM1 predict a shift of the CO stretch to lower wavenumber than free CO, while the ab initio results give a shift to higher wavenumber. Although our experimental data would seem to be more consistent with the MNDO/AM1 results, which give a lower CO stretching wavenumber for the adduct than that of carbon monoxide, we cannot decide from experimental evidence alone what the structure of the adduct is. A silacyclopentanone structure is computed to lie higher in energy by both AM1 and ab initio calculations. A more complete computational study of the H_2SiCO system is being undertaken by Hamilton and Schaefer at the University of Georgia.

The possibility that the carbon monoxide bonds to dimethylsilylene through the oxygen rather than the carbon is unlikely on the basis of calculated energies. MNDO calculations give a barrier of about 8 kJ/mol for the oxygen attachment to give a product that is less stable than the ketene by about 200 kJ/mol . Ab initio calculations indicate a similar preference for bonding through the carbon.

Acknowledgment. We gratefully acknowledge support of this work by grants from Research Corporation, the National Science Foundation, the Pew Memorial Trust, and the Charles A. Dana Foundation.

Registry No. **1**, 4098-30-0; **2**, 4774-73-6; CO, 630-08-0; ^{13}CO , 1641-69-6; C^{18}O , 4906-87-0; $(\text{CH}_3)_2\text{Si}^{12}\text{CO}^{16}\text{O}$, 115591-59-8; $(\text{CH}_3)_2\text{Si}^{13}\text{C}^{16}\text{O}$, 115591-60-1; $(\text{CH}_3)_2\text{Si}^{12}\text{C}^{18}\text{O}$, 115591-61-2; H_2SiCO , 109284-39-1; $(\text{CH}_3)_2\text{Si}$, 6376-86-9.

Ligand Field Transitions and the Origin of Zero Field Splitting in $[\text{PPh}_4][\text{FeCl}_4]$ and $[\text{NEt}_4][\text{Fe}(\text{SR})_4]$ ($\text{R} = 2,3,5,6\text{-Me}_4\text{C}_6\text{H}$): A Model for the High-Spin Fe(III) Site in Rubredoxin

Joseph C. Deaton,^{1a} Matthew S. Gebhard,^{1a}
Stephen A. Koch,^{1b} Michelle Millar,^{1b} and
Edward I. Solomon^{*,1a}

Department of Chemistry, Stanford University
Stanford, California 94305

Department of Chemistry, State University of New York at
Stony Brook, Stony Brook, New York 11794

Received April 4, 1988

Rubredoxin (Rb) is the simplest Fe–S center, containing an approximately D_{2d} distorted T_d Fe coordinated by four cysteines.² Geometric and electronic structure/function relationships for Rb have been investigated experimentally^{2–17} and theoretically.^{18–20}

(1) (a) Department of Chemistry, Stanford University, Stanford CA 94305. (b) Department of Chemistry, SUNY Stony Brook, Stony Brook NY 11794.

(2) (a) Watenpaugh, K. D.; Sieker, L. C.; Jensen, L. H. *J. Mol. Biol.* **1979**, *131*, 509–522. (b) Watenpaugh, K. D.; Sieker, L. C.; Jensen, L. H. *J. Mol. Biol.* **1980**, *138*, 615–633.

(3) (a) *Iron-Sulfur Proteins*; Lovenberg, W., Ed.; Academic Press: 1973; Vol. I and II. (b) *Iron-Sulfur Proteins*; Lovenberg, W., Ed.; Academic Press: 1977; Vol. III. (c) *Metal Ions in Biology Vol. IV Iron-Sulfur Proteins*; Spiro, T. G., Ed.; Wiley-Interscience: 1982.

(4) Muraoka, T.; Nozawa, T.; Hatano, M. *Inorg. Chem. Acta*, **1986**, *124*, 49–53.

(5) Rivoal, J. C.; Briat, B.; Cammock, R.; Hall, D. O.; Rao, K. K.; Douglass, I. N.; Thompson, A. J. *Biochem. Biophys. Acta* **1977**, *493*, 122–131.

(6) Bennett, D. E.; Johnson, M. K. *Biochem. Biophys. Acta* **1987**, *911*, 71–80.

(7) Shulman, R. G.; Eisenberger, P.; Teo, B. K.; Kincaid, B. M.; Brown, G. S. *J. Mol. Biol.* **1978**, *124*, 305–321.

(8) Long, T. V.; Loehr, T. M. *J. Am. Chem. Soc.* **1970**, *92*, 6384–6386.

(9) Long, T. V.; Loehr, T. M.; Allkins, J. R.; Lovenberg, W. *J. Am. Chem. Soc.* **1971**, *93*, 1809–1811.

(7) Vancik, H.; Raabe, G.; Michalczyk, M. J.; West, R.; Michl, J. *J. Am. Chem. Soc.* **1985**, *107*, 4097.

(8) (a) Stewart, J. J. P. *QCPE* no. 455 (Version 4.0). (b) Frisch, M. J.; Binkley, J. S.; Schlegel, H. B.; Ragavachari, K.; Melius, C. F.; Martin, R. L.; Stewart, J. J. P.; Bobrowicz, F. W.; Rohlfing, C. M.; Kahn, L. R.; Defrees, D. J.; Seeger, R.; Whiteside, R. A.; Fox, D. J.; Fleuder, E. M.; Pople, J. A. *GAUSSIAN 86*, Carnegie-Mellon Quantum Chemistry Publishing Unit, Pittsburgh, PA, 1984.

(9) Schaefer, H. F. *Acc. Chem. Res.* **1982**, *15*, 283.

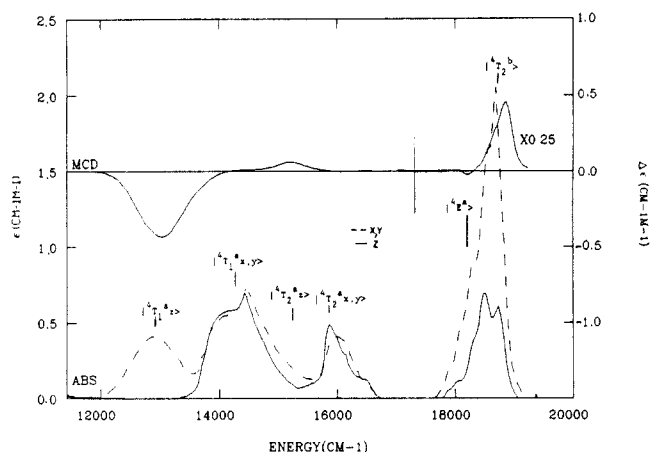


Figure 1. Polarized single crystal absorption and MCD spectra of $[\text{FeCl}_4][\text{PPh}_4]$. The polarized absorption is at 6 K for a 2.1-mm thick crystal. The MCD is at 2 K and 60 kG for a 500 μm thick crystal.

However, spectroscopic studies^{4,5,14-17} of oxidized Rb and related model compounds have not elucidated ligand field (LF) transitions, which probe Fe-S bonding, and are proposed²¹ to correlate to ground state (6A_1) zero field splitting (ZFS). We report the assignment of LF transitions, for a Rb model complex $(\text{Fe}(\text{SR})_4)^-$ $R = 2,3,5,6\text{-Me}_4\text{C}_6\text{H}$, with single crystal polarized absorption and magnetic circular dichroism (MCD). We also experimentally test Griffith's ZFS model.²¹ Comparison to parallel experiments on a D_{2d} FeCl_4^- complex reveals differences in these sites relating to covalent reduction of LF transition energies and effects of covalent anisotropy on D.

$[\text{FeCl}_4][\text{Ph}_4\text{P}^+]$ was prepared by adding concentrated HCl - (aqueous) to anhydrous FeCl_3 and precipitation with Ph_4P^+ . $[\text{Fe}(\text{SR})_4][\text{NEt}_4]$ was made by the procedure of Millar and Koch.^{22,23} Both salts crystallize in $I\bar{4}$ with Fe^{3+} at a 4 site. D was determined by EPR temperature dependence on isomorphous Ga analogues doped with 0.1% $\text{Fe}(\text{III})$.²⁵

Figure 1 shows polarized absorption and MCD spectra for FeCl_4^- , which combined with transverse Zeeman experiments²⁶ allow a definitive assignment of the LF spectrum of FeCl_4^- . This requires application of the irreducible tensor method²⁷ in D_{2d} symmetry to determine selection rules for spin forbidden $^6A_1 \rightarrow$

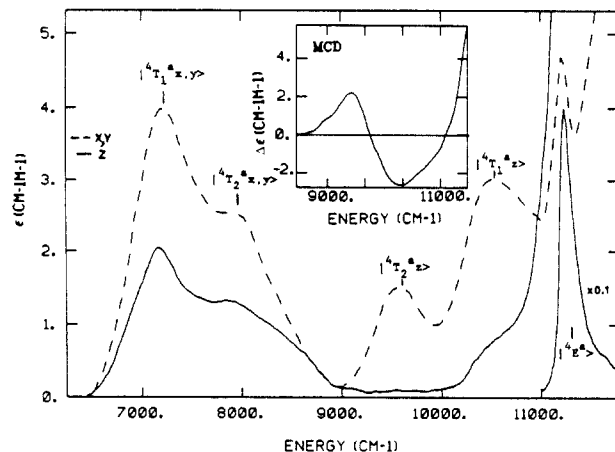


Figure 2. Polarized single crystal absorption and MCD spectra of $[\text{Fe}(\text{SR})_4][\text{NEt}_4]$ ($R = 2,3,5,6\text{-Me}_4\text{C}_6\text{H}$). The polarized absorption is at 2 K on 700 μm and 100 μm (11 235- cm^{-1} band in z polarization) thick crystals. The MCD (inset) is at 2 K and 60 kG on a 280 μm thick crystal.

4T LF transitions. In T_d symmetry, the excited states in order of increasing energy²⁸ are $^4T_1^a$, $^4T_2^a$, $^4E^a$, and $^4T_2^b$. The D_{2d} distortion splits the $^4T_1^a$ and $^4T_2^a$ states into z and x,y components. On the basis of their pure x,y polarization and respective negative and positive MCD, the 12 890 and 15 210 cm^{-1} transitions are assigned as $^4T_1^a(z)$ and $^4T_2^a(z)$. The mixed polarization of the 14 240 and 16 050 cm^{-1} transitions identifies these as $^4T_1^a(x,y)$ and $^4T_2^a(x,y)$, respectively. The transitions at 18 200 and 18 800 cm^{-1} are assigned as $^4E^a$ and $^4T_2^b$, based on their respective negative and positive MCD.

Griffith²¹ derived the following expression which relates the 6A_1 D to axial splitting of 4T_1 states

$$D = 1/180[(\langle ^4T_1z || H_{\text{so}} || ^6A_1 \rangle^2 / E_z) - (\langle ^4T_1xy || H_{\text{so}} || ^6A_1 \rangle^2 / E_{xy})] \quad (1)$$

where E_z and E_{xy} are energies of z and xy components of the 4T_1 . Evaluation of the spin orbit matrix elements in T_d symmetry gives,

$$D = ((\zeta_{\text{Fe}^{3+}})^2 / 5)[1/E_z - 1/E_{xy}] \quad (2)$$

where $\zeta_{\text{Fe}^{3+}}$ is the $\text{Fe}(\text{III})$ spin orbit coupling constant (430 cm^{-1}). There are three LF 4T_1 states (a , b , c) contributing to D . The $^4T_1^az$ and $^4T_1^ax,y$ are assigned in Figure 1, while the other 4T_1 's are calculated²⁹ from the Tanabe-Sugano matrices.²⁸ From eq 2 we get $D(\text{FeCl}_4^-)_{\text{calcd}} = +0.22 \text{ cm}^{-1}$, while $D(\text{FeCl}_4^-)_{\text{exp}} = -0.04 \text{ cm}^{-1}$. Thus the Griffith model predicts the wrong sign and magnitude of D . Equation 2 was derived assuming the matrix elements in eq 1 are equal. However, covalency effects in D_{2d} can, in fact, cause these to be different. In order to account for this, we derived²⁶ the following matrix elements which include covalent mixing of metal "d" orbitals

$$\langle ^4T_1^{(a,c)}z || H_{\text{so}} || ^6A_1 \rangle = 6(1 - \alpha^2)^{1/2}(1 - \beta^2)^{1/2}\zeta_{\text{Fe}^{3+}} + i(6)^{1/2}\alpha\beta\zeta_{\text{Cl}^-} \quad (3)$$

$$\langle ^4T_1^{(a,c)}xy || H_{\text{so}} || ^6A_1 \rangle = 6(1 - \alpha^2)^{1/2}(1 - \gamma^2)^{1/2}\zeta_{\text{Fe}^{3+}} + i(6)^{1/2}\alpha\gamma\zeta_{\text{Cl}^-} \quad (4)$$

$$\langle ^4T_1^{(b)}z || H_{\text{so}} || ^6A_1 \rangle = -(18)^{1/2}(1 - \gamma^2)\zeta_{\text{Fe}^{3+}} \quad (5)$$

$$\langle ^4T_1^{(b)}xy || H_{\text{so}} || ^6A_1 \rangle = -(18)^{1/2}(1 - \gamma^2)^{1/2}(1 - \beta^2)^{1/2}\zeta_{\text{Fe}^{3+}} \quad (6)$$

where α^2 , β^2 , and γ^2 represent the ligand character in the $d_{x^2-y^2}$, d_{xz} , and d_{yz} orbitals respectively, and ζ_{Cl^-} is the Cl^- spin orbit coupling constant (580 cm^{-1}). Application of eq 2-6 demonstrates that D_{exp} requires anisotropic covalency ($\beta^2 \neq \gamma^2$) in the t_2 set of "d" orbitals. A SCF-X α calculation³⁰ for the T_d site gives α^2

(28) Tanabe, Y.; Sugano, S. *J. Phys. Soc. Jpn.* **1954**, *9*, 753-779.

(29) With $Dq = -654 \text{ cm}^{-1}$, $B = 443 \text{ cm}^{-1}$, and $C = 2728 \text{ cm}^{-1}$ we get $\langle ^4T_1^{(a)}z || H_{\text{so}} || ^6A_1 \rangle = 12980$, $\langle ^4T_1^{(a)}xy || H_{\text{so}} || ^6A_1 \rangle = 14240$, $\langle ^4T_1^{(b)}z || H_{\text{so}} || ^6A_1 \rangle = 25990$, $\langle ^4T_1^{(b)}xy || H_{\text{so}} || ^6A_1 \rangle = 25990$, $\langle ^4T_1^{(c)}z || H_{\text{so}} || ^6A_1 \rangle = 30650$, and $\langle ^4T_1^{(c)}xy || H_{\text{so}} || ^6A_1 \rangle = 29300 \text{ cm}^{-1}$.

(10) Yachandra, V. K.; Hare, J.; Moura, I.; Spiro, T. G. *J. Am. Chem. Soc.* **1983**, *105*, 6455-6461.

(11) Czernuszewicz, R. S.; LeGall, J.; Moura, I.; Spiro, T. G. *Inorg. Chem.* **1986**, *25*, 696-700.

(12) Peisach, J.; Blumberg, W. E.; Lode, E. T.; Coon, M. J. *J. Biol. Chem.* **1971**, *246*, 5877-5881.

(13) Phillips, W. D.; Poe, M.; Weihler, J. F.; McDonald, C. C.; Lovenberg, W. *Nature (London)* **1970**, *227*, 574-578.

(14) Thompson, C. L.; Jackson, P. J.; Johnson, C. E. *Biochemistry J.* **1972**, *129*, 1063-1068.

(15) Eaton, W. A.; Lovenberg, W. In *Iron-Sulfur Proteins*; Academic Press: Vol. II, pp 131-162.

(16) Eaton, W. A.; Lovenberg, W. *J. Am. Chem. Soc.* **1970**, *92*, 7195-7198.

(17) Lane, R. W.; Ibers, J. A.; Frankel, R. B.; Papaefthymiou, G. C.; Holm, R. H. *J. Am. Chem. Soc.* **1977**, *99*, 84-98.

(18) Bair, R. A.; Goddard, W. A. III. *J. Am. Chem. Soc.* **1978**, *100*, 5669-5676.

(19) Noodleman, L.; Norman, J. G.; Osborne, J. H.; Aizman, A.; Case, D. A. *J. Am. Chem. Soc.* **1985**, *107*, 3418-3426.

(20) Norman, J. G., Jr.; Jackels, S. C. *J. Am. Chem. Soc.* **1975**, *97*, 3833-3835.

(21) Griffith, J. S. *The Theory of Transition-Metal Ions*; Cambridge University Press: 1964.

(22) Maelia, L. E.; Koch, S. A. *Inorg. Chem.* **1986**, *25*, 1896-1904.

(23) Millar, M.; Lee, J. F.; Koch, S. A.; Fikar, R. *Inorg. Chem.* **1982**, *21*, 4105-4106.

(24) Cotton, F. A.; Murillo, C. A. *Inorg. Chem.* **1975**, *14*, 2467-2469.

(25) Note that due to the strict axial symmetry for the Fe site, $E/D = 0$.

(26) Deaton, J. C.; Gebhard, M. S.; Solomon, E. I., to be published.

(27) Griffith, J. S. *The Irreducible Tensor Method for Molecular Symmetry Groups*; Prentice Hall: 1962.

$= 0.16$, and $\beta^2 = \gamma^2 = 0.27$. Varying the difference between β^2 and γ^2 to fit D_{exp} gives $\beta^2 = 0.30$ and $\gamma^2 = 0.25$. Thus, d_{xy} is more covalent than $d_{xz,yz}$, consistent with the flattened D_{2d} geometry.²⁴

Polarized absorption and MCD for the ligand field region of $\text{Fe}(\text{SR})_4^-$ are presented in Figure 2. By using the FeCl_4^- methodology, we make the following band assignments: 7250 cm^{-1} ($^4T_1^a(x,y)$); 7975 cm^{-1} ($^4T_2^a(x,y)$); 10525 cm^{-1} ($^4T_1^a(z)$); and 9540 cm^{-1} ($^4T_2^a(z)$). On the basis of bandshape and temperature dependence of the z polarized intensity,³¹ the 11225 cm^{-1} transition is assigned as the LF independent $^4E^a$.

Application of eq 2 with the experimental $^4T_1^a z$ and x,y energies gives $D(\text{Fe}(\text{SR})_4^-)_{\text{calcd}} = -1.6 \text{ cm}^{-1}$, while $D(\text{Fe}(\text{SR})_4^-)_{\text{exp}} = +2.5 \text{ cm}^{-1}$. Again, D_{exp} requires anisotropic covalency, but now $\gamma^2 > \beta^2$. Although the FeS_4 core has the same geometry²³ as FeCl_4^- , it has the opposite anisotropic covalency. This difference results from the C-S-Fe angle²³ of 102.4° , which rotates the S p - σ orbitals off the bond axis and toward the xz and yz planes.

A striking feature of $d \rightarrow d$ transitions in $\text{Fe}(\text{SR})_4^-$ is their low energy. This is attributed to drastic covalent reduction in electron repulsion,^{32,33} which lowers the energy of all states. In the absence of covalency, the $^4E^a$ should occur at the free ion 4G energy (32300 cm^{-1});³⁴ however, our FeCl_4^- data indicate a 44% reduction in this energy. For the ferric thiolate an intriguing 65% reduction is observed. This reduction provides strong evidence for a highly delocalized bonding scheme, consistent with calculations on related $\text{Fe}(\text{SR})_4$ models.¹⁸⁻²⁰

Acknowledgment. We thank the National Science Foundation Grant No. CHE-8613376 (E.I.S.) and the National Institute of Health Grant No. GM-36308 (M.M.) and GM-31849 (S.A.K.) for support of this research. M.S.G. and J.C.D. acknowledge NSF for graduate research fellowships.

Registry No. $[\text{FeCl}_4][\text{PPh}_4]$, 30862-67-0; $[\text{Fe}(\text{S}-2,3,5,6\text{-Me}_4\text{C}_6\text{H})_4][\text{NEt}_4]$, 82741-95-5.

(30) Butcher, K. D.; Didziulis, S. V.; Solomon, E. I. results from SCF-X α calculations to be published.

(31) Gebhard, M. S.; Deaton, J. C.; Solomon, E. I., to be published.

(32) Ferguson, J. *Prog. Inorg. Chem.* **1970**, *12*, 195-293.

(33) Jorgensen, C. K. *Prog. Inorg. Chem.* **1962**, *4*, 73-124.

(34) Reader, J.; Sugar, J. J. *Phys. Chem. Ref. Data* **1975**, *4*, 397-400.

Nonequilibrated Multiple Luminescence from $\text{CpRe}(\text{CO})_2(4\text{-Phpy})$ in 293 K Solution

Marsha M. Glezen and Alistair J. Lees*

Department of Chemistry, University Center at Binghamton
State University of New York
Binghamton, New York 13901

Received May 5, 1988

Multiple-state emission is a topic of current investigation and has now been clearly established for a number of transition-metal compounds.¹ A few systems even exhibit multiple emission in fluid solution, but in almost all cases the radiative excited states

have been shown to be thermally equilibrated.² Here we report the observation of nonequilibrated excited-state luminescence in room temperature solution for the organometallic complex $\text{CpRe}(\text{CO})_2(4\text{-Phpy})$ ($\text{Cp} = \eta^5\text{-C}_5\text{H}_5$; $4\text{-Phpy} = 4\text{-phenylpyridine}$). The photophysics of this system are especially unusual as distinct orbital emissions are readily observable in solution at 293 K.

Electronic absorption and emission data obtained from $\text{CpRe}(\text{CO})_2(4\text{-Phpy})$ and the closely related $\text{CpRe}(\text{CO})_2(\text{pip})$ ($\text{pip} = \text{piperidine}$) complex in deoxygenated benzene solutions at 293 K are shown in Figure 1. All the experimental results for both compounds, including emission quantum yields, lifetimes, excitation spectra, and low-temperature data, are summarized in Table I. The absorption spectrum of the $\text{CpRe}(\text{CO})_2(4\text{-Phpy})$ complex is dominated by two intense $\text{Re}(d\pi) \rightarrow (\pi^*)\text{L}$ metal-to-ligand charge-transfer (MLCT) transitions, which are referred to as the $\text{MLCT}(b_2)$ and $\text{MLCT}(e)$ bands; these transitions arise from degeneracy removal of the filled " t_{2g} " orbitals to yield levels of b_2 and e symmetry.⁵ Ligand field (LF) states are also present in $\text{CpRe}(\text{CO})_2(4\text{-Phpy})$ and appear as a high energy shoulder on the intense MLCT absorption envelope; the positions of these levels are more clearly depicted by the absorption spectrum of the $\text{CpRe}(\text{CO})_2(\text{pip})$ complex (see Figure 1).^{5,6}

The luminescence spectrum of $\text{CpRe}(\text{CO})_2(4\text{-Phpy})$ is striking as it exhibits three distinct maxima.⁷ The two lowest lying emission features are both solvent and temperature dependent and, therefore, are associated with the $^3\text{MLCT}(b_2)$ and $^3\text{MLCT}(e)$ excited states.^{8,9} A third weak emission band is observable at higher energy, but this exhibits relatively little solvent and temperature sensitivity and, consequently, is assigned to a ^3LF emission. Strong support for the ^3LF assignment is obtained from the room temperature emission data of the closely related $\text{CpRe}(\text{CO})_2(\text{pip})$ complex.^{6,9} Excitation spectra monitored at each of the luminescence maxima of both complexes are also concordant with these LF and MLCT assignments. Spectra obtained while monitoring emission of $\text{CpRe}(\text{CO})_2(4\text{-Phpy})$ at either MLCT maxima (542 or 710 nm) depict bands centered at 346, 402, and 450 nm, consistent with the LF and MLCT absorption positions (see Table I). On the other hand, monitoring at the high energy LF emission (440 nm) of $\text{CpRe}(\text{CO})_2(4\text{-Phpy})$ results in a single excitation maximum centered at 346 nm, indicating the LF absorption energy. The $\text{CpRe}(\text{CO})_2(\text{pip})$ complex exhibits a single excitation maximum at 344 nm, in accordance with the LF assignment.

The two lowest lying MLCT emitting states of $\text{CpRe}(\text{CO})_2(4\text{-Phpy})$ are apparently in thermal equilibrium under room temperature solution conditions because the observed decay lifetimes are identical for both emission bands.¹⁰ Additionally, the relative ratio of the emission band intensities remains constant

(2) (a) Watts, R. J. *Inorg. Chem.* **1981**, *20*, 2302. (b) Kirchhoff, J. R.; Gamache, R. E.; Blaskie, M. W.; Del Paggio, A. A.; Lengel, R. K.; McMillin, D. R. *Inorg. Chem.* **1983**, *22*, 2380. (c) Nishizawa, M.; Suzuki, T. M.; Sprouse, S.; Watts, R. J.; Ford, P. C. *Inorg. Chem.* **1984**, *23*, 1837.

(3) Parker, C. A.; Rees, W. T. *Analyst (London)* **1960**, *85*, 587.

(4) Van Houten, J.; Watts, R. J. *J. Am. Chem. Soc.* **1976**, *98*, 4853.

(5) Giordano, P. J.; Wrighton, M. S. *Inorg. Chem.* **1977**, *16*, 160.

(6) Glezen, M. M.; Lees, A. J. *J. Chem. Soc., Chem. Commun.* **1987**, 1752.

(7) Emission from a sample impurity is excluded on the basis that the luminescence spectrum is reproducible for different preparation and purification methods of the $\text{CpRe}(\text{CO})_2(4\text{-Phpy})$ complex. These procedures included synthesis by both thermal (carried out in complete darkness) and photochemical routes and purifications by vacuum sublimation, column chromatography, and recrystallization. Emission from a photochemically produced impurity is ruled out on the evidence that the emission spectral distribution is not affected on varying the irradiation time. Moreover, both the parent $\text{CpRe}(\text{CO})_3$ complex and the free ligands themselves exhibit no observable emission under identical experimental conditions.

(8) For a recent review on luminescence properties of organometallic complexes, see: Lees, A. J. *Chem. Rev.* **1987**, *87*, 711.

(9) Spin-orbit coupling in these heavy metal complexes precludes describing these states as "pure" triplets. See ref 8 for further discussion of this subject.

(10) Studies of the emission temperature dependence over the 213-293 K range are consistent with two close lying MLCT states in thermal equilibrium and not a thermal activation model; details of this work will be reported in a subsequent full paper.

(1) (a) For a review of literature appearing up to 1980, see: DeArmond, M. K.; Carlin, C. M. *Coord. Chem. Rev.* **1981**, *36*, 325. (b) Sullivan, B. P.; Abruna, H.; Finklea, H. O.; Salmon, D. J.; Nagle, J. K.; Meyer, T. J.; Sprintschnik, H. *Chem. Phys. Lett.* **1978**, *58*, 389. (c) Rader, R. A.; McMillin, D. R.; Buckner, M. T.; Matthews, T. G.; Casadonte, D. J.; Lengel, R. K.; Whittaker, S. B.; Darmon, L. M.; Lytle, F. E. *J. Am. Chem. Soc.* **1981**, *103*, 5906. (d) Martin, M.; Krogh-Jespersen, M.-B.; Hsu, M.; Tewksbury, J.; Laurent, M.; Viswanath, K.; Patterson, H. *Inorg. Chem.* **1983**, *22*, 647. (e) Belser, P.; von Zelewsky, A.; Juris, A.; Barigelletti, F.; Balzani, V. *Chem. Phys. Lett.* **1984**, *104*, 100. (f) Segers, D. P.; DeArmond, M. K.; Grutsch, P. A.; Kital, C. *Inorg. Chem.* **1984**, *23*, 2874. (g) Casadonte, D. J.; McMillin, D. R. *J. Am. Chem. Soc.* **1987**, *109*, 331. (h) Blakley, R. L.; DeArmond, M. K. *J. Am. Chem. Soc.* **1987**, *109*, 4895.